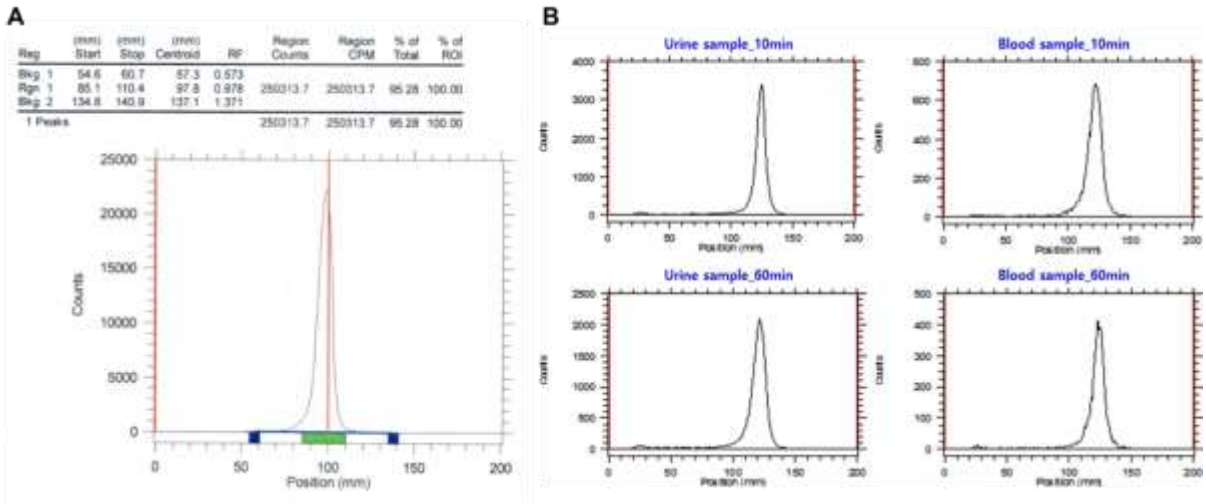

Supplemental Figure 1. Radiochemical purity was assessed according to the thin layer chromatography (TLC) method using 0.1 M sodium carbonate (Na_2CO_3) solution as a solvent with 1 μL of 68Ga-NGUL. The stability test of ^{68}Ga-NGUL was conducted at baseline, 1 hour, and 2 hours. pH was measured by dropping 1 μL of ^{68}Ga-NGUL on pH paper. Also, the TLC experiment was performed using urine and blood samples 10 minutes, 1 hour after the injection. The radiochemical purity of ^{68}Ga-NGUL was over 95% and remained stable until 2 hours at room temperature (A). pH was measured to be 4.7, this was a value that fits our preset criteria (pH 4 to 5). Furthermore, the radiochemical purities of the compound were over 99% in urine and blood samples which were obtained 10 minutes, 1 hour after the injection (B).

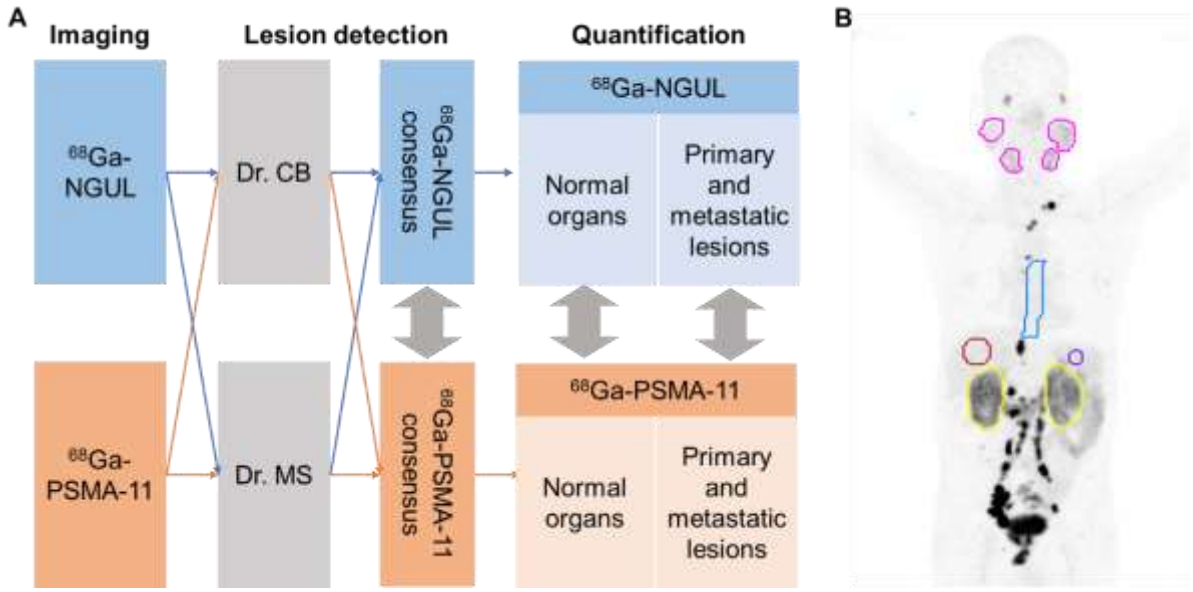

Supplemental Figure 2. Image acquisition and analysis

(A) Whole patients underwent whole-body static PET/CT imaging, 1 hour after an injection of PSMA targeting tracer with a mean dose of 130.2 ± 25.5 MBq (92.5 – 166.5 MBq). Emission scans were acquired at 2 min per bed using dedicated PET/CT scanners (Biograph mCT 64, Siemens Medical Solutions), followed by CT scans with 120kV and a CARE Dose 4D reference of 50mAs for attenuation correction. PET images were reconstructed by an iterative algorithm (ordered-subset expectation maximization, OSEM). Three patients underwent a dynamic study. Dynamic PET/CT scans were performed over the pelvic region for 60 minutes using a 28-frame protocol (10 frames of 30 s, 5 frames of 60 s, 5 frames of 120 s, and 8 frames of 300 s). Reconstruction parameters were identically applied as the static image. The images were reviewed on MIM software (MIM Encore^{TM}, MIM Software Inc., Cleveland, OH). All scans were reviewed separately by nuclear medicine physicians (CB, MS), masked to the patient medical history. Regarding the inconsistency, we reached a consensus afterward. Both scans were analyzed at a different time point. Any lesion in the prostate was considered as positive when the uptake was focal and higher than adjacent prostate tissue. Outside the prostate, a pathologic lesion was defined as any soft-tissue or skeletal lesion with focal uptake which is higher than normal adjacent tissue and not explained by physiologic uptake. Lesion numbers were counted for both ^{68}Ga-NGUL and ^{68}Ga-PSMA-11. For the quantitative analysis, SUV_{max} of all lesions, up to a maximum of five lesions total (and a maximum of two lesions per organ) with the most intense tracer uptake, were estimated in each patient. The tumor-to-background ratio was measured based on the ratio of tumor SUV_{max} and the gluteal muscle SUV_{mean} reflecting the background activity. (B) Normal tissue distribution was compared in the inferior vena cava and the following organs: major salivary glands,

liver, spleen, and kidney. The volume of interest was applied to major salivary glands and kidneys using a gradient-based segmentation method (PET Edge). Spherical volume of interest was drawn on the liver and spleen. For the evaluation of inferior vena cava, circular regions of interests were drawn on every 5-mm axial image and interpolated to acquire a single volume of interest, from the liver tip to the subcarinal level. In addition, spherical volume of interest was applied to the gluteal muscle to estimate the background activity. The normal-organ distribution and blood pool activity of both tracers were quantified as SUV_{mean}. There was no visual evidence of tumor involvement in the target organs, where the volume of interest was drawn. In addition, three patients underwent dynamic PET scanning (60 min) of the pelvic region and lower abdomen to evaluate the urinary excretion by estimating bladder activity.

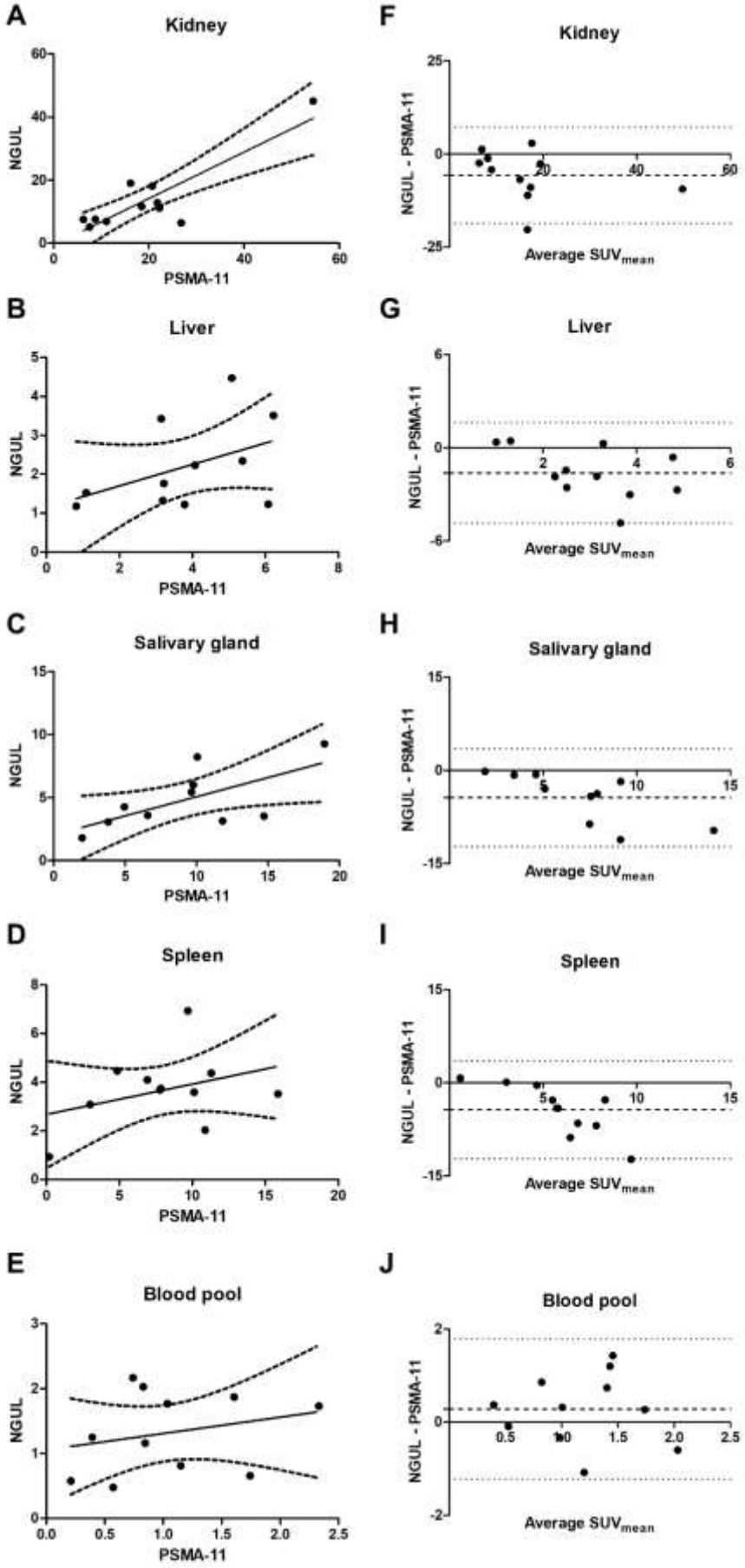
A
Kidney
NGUL
PSMA-11
B
Liver
NGUL
PSMA-11
C
Salivary gland
NGUL
PSMA-11
D
Spleen
NGUL
PSMA-11
E
Blood pool
NGUL
PSMA-11
F
Kidney
NGUL - PSMA-11
Average SUVmean
G
Liver
NGUL - PSMA-11
Average SUVmean
H
Salivary gland
NGUL - PSMA-11
Average SUVmean
I
Spleen
NGUL - PSMA-11
Average SUVmean
J
Blood pool
NGUL - PSMA-11
Average SUVmean

Suh et al.

Supplemental Figure 3. Correlation and agreement between ^{68}Ga-NGUL and ^{68}Ga-PSMA-11 in normal organs

(A-E) Scatter plot of SUV_{mean} showing the correlation between ^{68}Ga-PSMA-11 and ^{68}Ga-NGUL in each normal organ. In the kidney, both tracers showed good correlation, whereas, other organs showed a fair to poor correlation between two tracers. Regression line and 95% CI were plotted. (F-J) Bland-Altman plot showing the difference of SUV_{mean} between ^{68}Ga-PSMA-11 and ^{68}Ga-NGUL, according to their average. Bland-Altman analysis revealed proportional bias in the salivary gland and spleen. Here the difference between ^{68}Ga-NGUL and ^{68}Ga-PSMA-11 uptake increased as the average activity increased. Blood pool activity showed no significant difference between the two tracers. Accordingly, an acceptable agreement with a mean bias of 0.3±0.7 was observed in the blood pool. Dotted lines represent the mean bias and 95% limits of agreement.

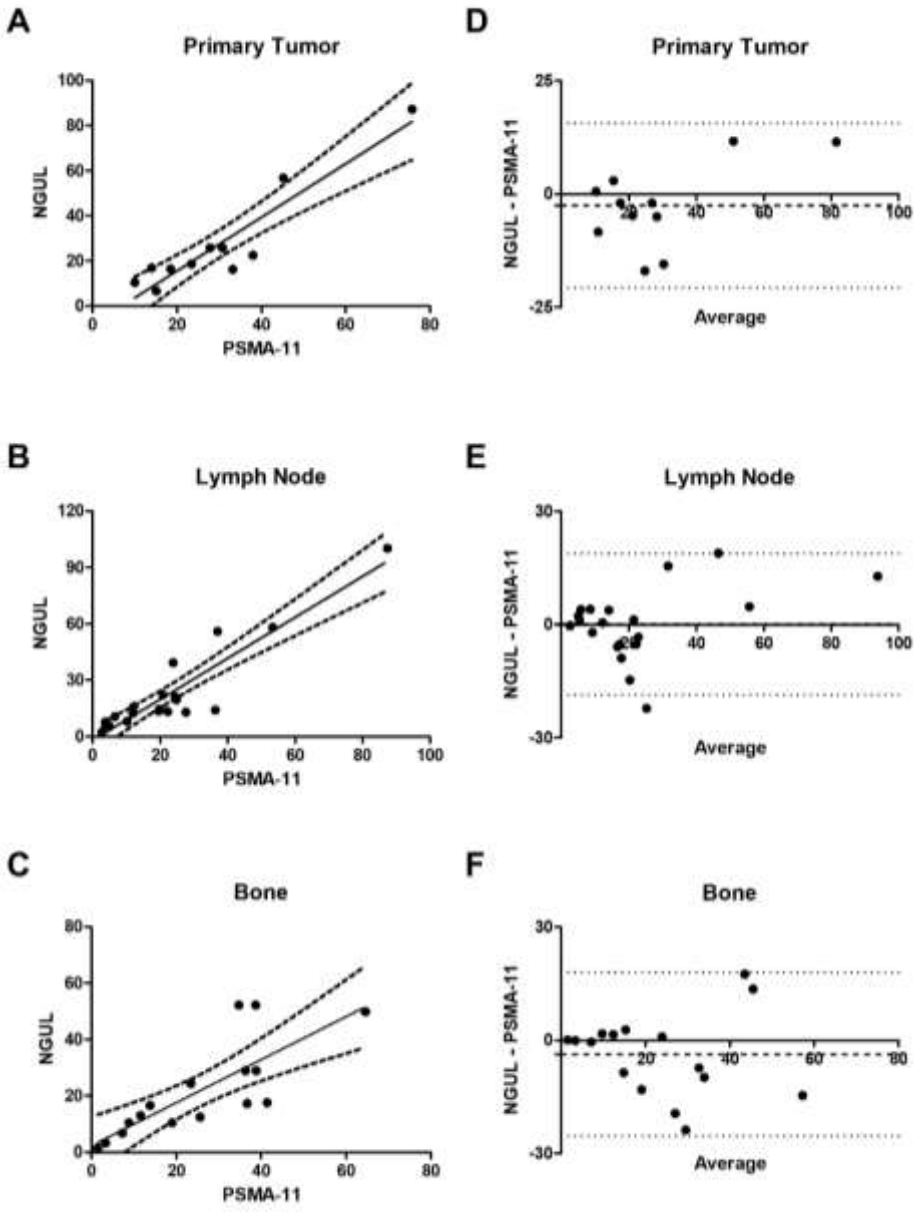

Supplemental Figure 4. Correlation and agreement between ^{68}Ga-NGUL and ^{68}Ga-PSMA-11 in primary and metastatic lesions

(A-C) Scatter plot of SUV_{max} showing the correlation between ^{68}Ga-PSMA-11 and ^{68}Ga-NGUL in the primary tumor, lymph node metastases, and bone metastases. The quantitative primary tumor uptake showed good correlation between ^{68}Ga-NGUL and ^{68}Ga-PSMA-11 (R^2 = 0.910, $p < 0.001$). The quantified uptake in metastatic lesions of both tracers showed a good correlation with R^2 of 0.845 in lymph node metastases and 0.624 in bone metastases. Regression line and 95% CI were plotted. (D-F)

Bland-Altman plot showing the difference of SUV_{max} between ^{68}Ga-PSMA-11 and ^{68}Ga-NGUL, according to their average. The two tracers had an acceptable overall agreement with a calculated mean bias of -3.2 ± 7.2 for the primary tumor, -1.5 ± 10.2 for lymph node metastases, and -4.8 ± 11.2 for bone lesions. Dotted lines represent the mean bias and 95% limits of agreement.

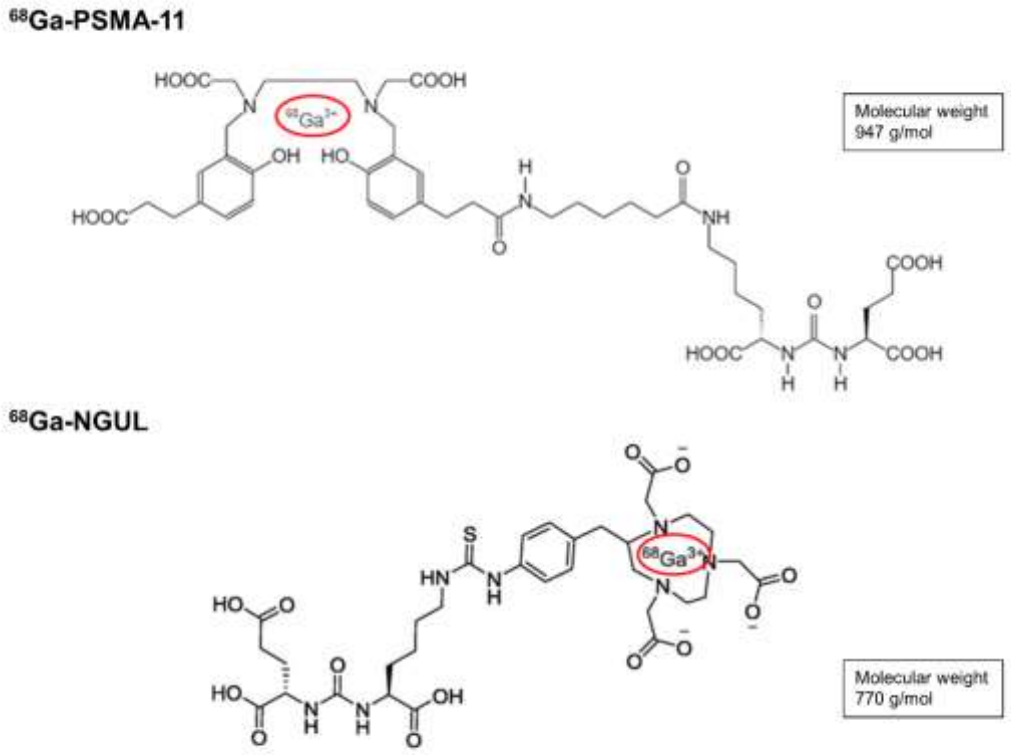

Supplemental Figure 5. Radiolabeling and chemical structure of ^{68}Ga-NGUL and ^{68}Ga-PSMA-11

The radiolabeling of ^{68}Ga-PSMA-11 was performed over 5 minutes using a disposable cassette, labeling kit, and 10ug of precursor, PSMA-HBED-CC (ABX GmBH, Radeberg, Germany) dissolved in 1 mL of sodium acetate buffer (0.25 M). ^{68}Ga-NGUL was prepared similarly to the previous study (*Bioorg Med Chem*. 2018;26:2501-2507). Briefly, $^{68}GaCl_3$ in 0.1 M HCl solution was added to the NGUL kit vial (Cellbion, Seoul, Korea). The vial was vigorously mixed for 1 min and then was incubated for 10 min at room temperature.

Supplemental Table 1. Characteristics of patients (n=11)

	Age	Time gap between both scans (day)	PSA (ng/ml)	Gleasons Score	Local Treatment	Chemotherapy	Hormonal Therapy	Disease State
1	69	1	1.8	N/A	Not done	Not done	Done	HSPC
2	67	4	94.8	4+3	Not done	Done	Done	CRPC
3	67	1	184.6	3+4	TURP	Not done	Done	HSPC
4	70	4	N/A	4+3	Not done	Not done	Done	HSPC
5	72	2	N/A	N/A	Not done	Not done	Done	HSPC
6	50	4	151.0	4+4	Not done	Not done	Done	HSPC
7	55	1	28.3	N/A	Radiotherapy	Done	Not done	CRPC
8	84	1	1.7	3+5	Not done	Not done	Done	HSPC
9	63	1	1462.9	4+5	Not done	Done	Done	CRPC
10	80	2	63.7	3+3	TURP	Not done	Done	HSPC
11	67	4	52.2	4+5	Not done	Done	Not done	CRPC
Median (Range)	**67 (50-84)**	**2 (1-4)**	**63.7 (1.8-1462.9)**					

Supplemental Table 2. Comparison of quantitative values between ^{68}Ga-NGUL and ^{68}Ga-PSMA-11

Target Organ	**NGUL SUV_{mean}** Median (ICR)	**PSMA-11 SUV_{mean}** Median (ICR)	**Paired test p value**	**Linear Regression** R^2	p value	**Bland-Altman** Mean Bias (SD)
Kidney	11.6 (7.8-17.2)	20.7 (10.1-23.1)	0.005	0.775	< 0.001	-6.3 (6.2)
Liver	1.8 (1.5-3.2)	4.0 (3.4-5.3)	0.005	0.184	0.188	-1.8 (1.6)
Salivary gland*	4.4 (3.1-6.9)	9.9 (4.9-12.2)	0.002	0.489	0.024	-4.7 (3.7)
Spleen	3.7 (3.2-4.6)	9.7 (6.3-10.7)	0.005	0.294	0.085	-4.7 (3.9)
Blood pool	1.3 (0.8-1.8)	0.9 (0.8-1.5)	0.240	0.076	0.413	0.3 (0.7)
Target Lesion	**NGUL SUV_{max}**	**PSMA-11 SUV_{max}**				
Primary Tumor	18.7 (16.4-31.8)	27.8 (17.9-38.7)	0.102	0.910	< 0.001	-3.2 (7.2)
Lymph Node	14.8 (10.5-24.8)	20.3 (9.2-26.2)	0.674	0.841	< 0.001	-1.5 (10.2)
Bone	19.6 (11.5-29.0)	24.5 (11.4-37.7)	0.175	0.697	< 0.001	-4.8 (11.2)

*Number of the case is 10, since the scan coverage was limited to the lower neck level

ICR: Interquartile range, SD: Standard deviation

Supplemental Table 3. Visual analysis of lesion number

Patient	Primary Tumor		Lymph Node		Bone		Total	
	NGUL	PSMA-11	NGUL	PSMA-11	NGUL	PSMA-11	NGUL	PSMA-11
1	Yes	Yes	5	5	13	13	18	18
2	Yes	Yes	27	27	12	12	39	39
3	Yes	Yes	4	4	23	23	27	27
4	Yes	Yes	12	12	disseminated	disseminated	12	12
5	Yes	Yes	14	14	disseminated	disseminated	14	14
6	Yes	Yes	8	8	8	8	16	16
7	Yes	Yes	13	13	0	0	13	13
8	Yes	Yes	5	5	0	0	5	5
9	Yes	Yes	0	0	disseminated	disseminated	0	0
10	Yes	Yes	51	51	3	3	54	54
11	Yes	Yes	22	22	0	0	22	22
Sum	11	11	161	161	59	59	231	231

Supplemental Table 4. Dosimetry

In order to evaluate the in vivo distribution of ^{68}Ga-NGUL in normal BALB/c mice, blood and major organs were obtained at 15, 30 minutes and 1, 2, 4 hours after intravenous injection of ^{68}Ga-NGUL (185 kBq/100 μL) (n=4 for each time point). Biodistribution data was obtained by calculation of weight and radioactivity of the blood and major organs. The absorbed doses of organs and effective dose were calculated by extrapolating the biodistribution results obtained based on the mouse to a normal adult (70 kg), using the OLINDA/EXM program.

Target organ	Mean(mGy/MBq)
Intestine	0.0036
Stomach wall	0.0036
Heart wall	0.0126
Kidneys	0.2190
Liver	0.0023
Lungs	0.0038
Muscle	0.0016
Red marrow	0.0067
Osteogenic cells	0.0094
Spleen	0.0453
Effective dose	**0.019 (mSv/MBq)**